

Article

Assessment of State-Space Building Energy System Models in Terms of Stability and Controllability

V. S. K. V. Harish ^{1,*}, Arun Kumar ², Tabish Alam ^{3,*} and Paolo Blecich ^{4,*}

¹ Department of Electrical Engineering, Netaji Subhas University of Technology (NSUT), Sector-3, Dwarka, Delhi 110078, India

² Department of Hydro and Renewable Energy, Indian Institute of Technology Roorkee (IITR), Haridwar, Roorkee 247667, India; aheciitr.ak@gmail.com

³ CSIR-Central Building Research Institute, Roorkee 247667, India

⁴ Department of Thermodynamics and Energy Engineering, Faculty of Engineering, University of Rijeka, 51000 Rijeka, Croatia

* Correspondence: vskvharish@ieee.org (V.S.K.V.H.); tabish.iitr@gmail.com (T.A.); paolo.blecich@riteh.hr (P.B.)



Citation: Harish, V.S.K.V.; Kumar, A.; Alam, T.; Blecich, P. Assessment of State-Space Building Energy System Models in Terms of Stability and Controllability. *Sustainability* **2021**, *13*, 11938. <https://doi.org/10.3390/su132111938>

Academic Editor:
Ali Bahadori-Jahromi

Received: 27 August 2021

Accepted: 18 October 2021

Published: 28 October 2021

Publisher's Note: MDPI stays neutral with regard to jurisdictional claims in published maps and institutional affiliations.



Copyright: © 2021 by the authors. Licensee MDPI, Basel, Switzerland. This article is an open access article distributed under the terms and conditions of the Creative Commons Attribution (CC BY) license (<https://creativecommons.org/licenses/by/4.0/>).

1. Introduction

1.1. Background

The International Energy Agency has estimated about a 50% increase in the demand for energy in the buildings sector by 2060 [1]. Buildings, as a sector, are accountable for around one-third of total global energy use [2]. Several control strategies are being developed to improve the energy performance of buildings (of any functionality in the residential, commercial, municipal, and institutional sectors) [3,4]. Building automation, integrated with control strategies, enables the building owners and managers to achieve energy efficiency targets for green building ratings and standards [5]. In addition, the operational efficiency of buildings can be improved by changing the occupants' behavior and by developing improved energy control algorithms that consider active occupancy dynamics. Such considerations enable the building energy system (BES) to operate at an improved energy usage point without jeopardizing the safety and comfort of the occupants.

Energy modeling is a very important part of the building energy control design [6–9]. The development of a reliable and accurate building energy model is, thus, necessary in order to investigate the feasibility and performance of the energy control strategies. Reliability in the building energy model involves the inclusion of all the significant parameters

in model development, and the achievement of a response that is as close in approximation as possible to real-time experiments or standardized empirical results [10–12]. The American Society of Heating, Refrigerating and Air-Conditioning Engineers (ASHRAE), an intergovernmental organization headquartered in Georgia, the United States, enables the modelers and researchers to develop building energy simulation models using the test procedures laid out in the ANSI/ASHRAE Standard 140-2007 [13].

1.2. Literature Survey

Building energy system models can be categorized as white-box, black-box, and grey-box energy models, depending upon the availability of the experimental data [14,15]. White-box models are purely theoretical models that involve mathematical formulations of the energy transfer processes occurring within the building under consideration. The physical elements, such as the building envelope (walls, roof, floor, etc.), and the windows, shades, etc., are considered as single-layered or multilayered elements for developing building energy models [16,17]. Single-layered modeling has been mostly used to develop energy control strategies for heating, ventilation, and air-conditioning (HVAC) [18–20] and lighting systems [21,22].

The development of building energy models using multilayered construction elements improved the accuracy by taking into account the thickness, density, heat conductivity, and thermal capacity of each layer that constitutes a building element [23,24]. However, many studies report multilayer constructions that ignore the thermal air gaps within the construction elements. Control solutions developed for building energy systems, such as lighting, ventilation control, and blind control, etc., often become unstable when the system is simulated for a longer period of time [25,26]. A building energy model becomes unstable when excited by rapidly varying inputs and also because of unmodeled disturbances, such as outdoor environmental conditions, transient occupancy fluctuations, etc. This instability results in the occupants' discomfort and high-energy consumption. Building energy simulation programs have been developed for building energy system model development and analysis. The procedure adopted by building energy simulation programs for design and model development is shown in Figure 1 [27].

In the conceptual design phase, building energy simulation programs assist in optimal designing and modeling in order to achieve a high level of comfort for the occupants. However, the assessment of the stability to variable inputs, and the interactions between the state variables and the input parameters, is not conducted. The problems of ineffective control that arise in the later phases of the detailed design phase, postconstruction phase, and the operation and control phases can be prevented by conducting stability and controllability tests at the conceptual design phase [28]. The additional costs that are incurred during the maintenance and rectification of control problems at a later stage of the operation can, thus, be avoided.

The building energy system models developed so far use dynamic modeling and undergo simulations to test the detailed design, where the cost of error removal is high [29,30]. Such models have embedded conventional control techniques, such as on-off, PI, and PID control. As any particular building energy system is a MIMO system, identifying the factors responsible for the model's instability and parametric uncontrollability becomes a very tedious exercise. Moreover, this may lead to losses during the post-commissioning and operation phase, as there exists a large number of influential parameters [31]. Thus, during the design phase, it becomes imperative to conduct stability and controllability tests on the developed building energy system models and identify the extent of the state-input variable interactions (Table 1).

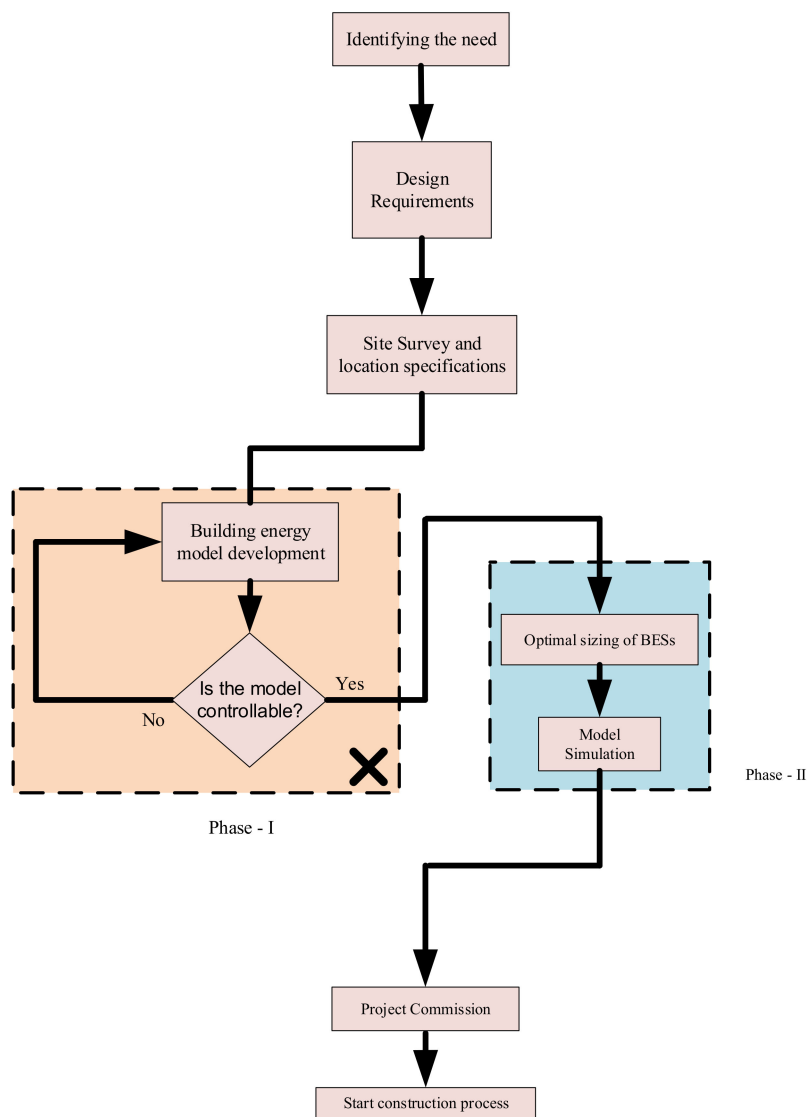


Figure 1. Significance of controllability studies in building energy modeling and design process (X: not included in current practice).

1.3. Gaps Identified

Very little research has been conducted on the stability studies and controllability assessments of building energy system models. Counsell et al., 2011, developed a full-scale building energy model of a school in Scotland using the climate-adaptive building philosophy [31]. Basic heat and mass transfer energy equations were used to develop a building energy model for a single zonal space. Mathematical expressions using ordinary differential equations governing the building space air temperature, lux-level, and CO₂ concentrations were developed.

Similar works are reported in [31,45], where building energy models were formulated as state-space equations. The structure and rank of the CB+sD matrix of the developed state-space model were observed in a root-locus analysis to determine the direction of the asymptotes and, hence, the stability. The effects of the outdoor parameters, such as the wind characteristics, temperature, and solar radiation, were not considered. The assessments were carried out for full-scale building energy system models, which increased the complexity of the developed building energy system model. The parameter of relative humidity was ignored.

Table 1. Summary of works in the field of Building Energy Control Systems.

Source	BES Components Under Study	Model Category	State Variables	Controllable Parameters	Occupancy Consideration	Simulation Period	Control Scheme ¹	Simulation Tool	Case Study Location
Pasichnyi et al., (2019) [32]	heat pumps and electric radiators	Grey-box	balance point temperature, total heat energy demand	power demand, electric heat consumption	Yes	Annual	Quasi linear regression analysis	RStudio IDE, DesignBuilder	Stockholm (Sweden)
Lamberti et al., 2021 [33]	building space air flow	Black-box	weather variables for various climatic zones	indoor air quality, thermal comfort	Yes	Variable	-	-	Multiple
Sim et al., 2021 [34]	solar thermal, ground source heat pump, solar PV	Grey-box	heating load, lighting load	building energy consumption	Yes	Annual	Multi objective Particle Swarm Optimization	MATLAB and DesignBuilder	Korea
Tsay et al., 2021 [35]	building envelope	Grey-box	climate zones, orientations, and insulation and glazing	life-cycle CO ₂	No	Annual	Gradient boosting decision tree based Machine Learning	EnergyPlus, SimaPro	Taiwan
Paneru et al., 2021 [36]	building envelope: an external wall	White-box	wall's material weight, density, thermal	weight (lb) and transformity (solaremjoule/lb)	No	-	-	Revit®2021 and MS Excel	None
Yang et al., 2020 [37]	HVAC system	Grey-box	building space air temperature, HVAC system load, relative humidity	PMV for thermal comfort	Yes	Annual	MPC	MATLAB optimization toolbox	Singapore
Homod et al., 2020 [38]	HVAC system	Grey-box	building space air temperature, nodal temperatures of building elements, relative humidity	PMV and PPD for thermal comfort	Yes	One-day	fuzzy PI-PD Mamdani-type controller	-	Iraq
Tang et al., 2021 [39]	central air-conditioning system	Black-box	occupant schedule, AHU power on/off state	energy consumption of chiller plant	Partial (occupancy schedule)	Daily, weekly	occupant-in-loop on/off control	-	Hong Kong
Peng et al., 2021 [40]	central air-conditioning system	Black-box	mean square error	power consumption	No	5 months	neural-network-based learning	-	Shenzhen, China

Table 1. *Cont.*

Source	BES Components Under Study	Model Category	State Variables	Controllable Parameters	Occupancy Consideration	Simulation Period	Control Scheme ¹	Simulation Tool	Case Study Location
Vasak et al., 2021 [41]	HVAC system	Grey-box	battery system state-of-energy, HVAC plant temperature	building temperature, occupants' comfort	Yes	24 h	MPC	Python with IBM CPLEX	Zagreb, Croatia
Zhao et al., 2020 [42]	HVAC system	Black-box	comfort parameters (PMV, temperature, humidity), energy/load	PMV (Fanger's model)	Yes	1 month	predictive control	Python	China
Sung and Ahn, 2020 [43]	HVAC system	White-box	temperature and relative humidity	PPD	Yes	2 days	on-demand and predictive control	EnergyPlus	Xuzhou, China
Lou et al., 2020 [44]	thermostat of air-conditioner	Black-box	room temperature, humidity, inferred thermostat measurement, metabolic rate	PMV (Fanger's model)	No	1 day	data-driven feedback control	MATLAB 2019a	USA
Campisi et al., 2018 [15]	heating load	Black-box	thermal energy transfer rate within the building space	energy requirements for heating	No	Annual	multi criteria decision analysis	-	Lecce, Italy
Shamsi et al., 2021 [24]	HVAC system	Grey-box	weather variables, internal temperature profiles,	building space heat demand	Yes	4 weeks	analysis of variance test	Energy Plus	San Francisco, USA

¹: MPC: Model Predictive Control; PI: Proportional-Integral Control, PD: Proportional Derivative Control. PMV: Predictive Mean Vote; PPD: Predicted Percentage of Dissatisfied.

The building energy models reported in the literature have been developed for assessing the energy performance of building energy systems, rather than for assessing the stability and controllability of the system against the servicing parameters, such as building space air temperature, air relative humidity, luminance, and indoor air quality. Moreover, building energy systems are MIMO systems with several energy transfer interactions occurring within and outside the system. Precise and computationally efficient building energy system models are required in order to effectively assess the controllability and stability of the servicing parameters. Some studies have used mechanical ventilation for controlling CO₂ concentration levels only and have ignored the cooling aspect.

The present study aims to find potential solutions and explore answers to questions such as:

- (Q1) *In which step of building energy model development can one assess for variables in model simulation that can be controllable or not?*
- (Q2) *How can the stability of a building energy system model be tested?*
- (Q3) *How can we investigate both the stability and the controllability of an integrated building energy system model?*
- (Q4) *What framework/approach should exist to investigate the input to state interaction for building energy system models?*

1.4. Significant Contributions of the Paper

In this paper, the concepts of stability and controllability are investigated for the energy system models of building. The energy plant taken into consideration for this study is an HVAC system. Controllability assessment studies were conducted for a range of setpoint values. Passive energy control and comfort management strategies were not considered in this study. A methodology for conducting stability and controllability assessment tests on the building energy model is proposed using inverse dynamics input theory (IDIT) [46,47]. The present study extends the work published in [23,48]. The building energy system model is represented in state-space form in order to understand the interactions between the building space variables (both outdoor and indoor), such as air temperature, humidity, occupancy, and other causal thermal gains and state variables, such as the nodal temperatures of the building elements, HVAC heating/cooling load, and lighting system load.

A white-box single zonal mathematical building energy system model was developed in MATLAB/Simulink. Lumped capacitance (RC) network models were considered for the building construction elements, such as the walls, roof, etc. IDIT was adopted for the controllability assessment test because of its ability to study a MIMO system as a number of SISO systems with reduced complexity and less, or no, loss of information. The strategy developed in this paper characterizes the important properties of building energy systems through the analysis of the state-equation data (namely, the coefficient matrices A , B , C , and D using IDIT). Tracking the trajectory of how control variables are influenced by state variables for building energy system models may assist the building designers, energy control engineers, retrofitters, and managers in order to improve the procedure for developing energy control strategies for the building industry. A similar approach can be applied to low-, medium-, and high-thermal capacity buildings. As the input-to-state trajectory of the energy system variables can be assessed for stability and controllability, designers can be guided for both the slow and fast actuation of HVAC systems. The approach developed in this paper may also generate interest in conducting energy control research in order to assess the developed energy system models before developing and applying any energy control strategies.

The remainder of this paper is categorized as follows: Section 2 introduces the basic concepts of the stability and controllability tests for a linear time-invariant state-space model; Section 3 represents the methodology for analyzing the stability and assessing the controllability of the building energy system; the simulation results are presented in

Sections 4 and 5; Section 7 discusses the results in detail and points out the limitations; and Section 8 concludes the paper.

2. Concepts of Stability and Controllability

2.1. Stability

For a particular control model, stability is the most significant factor for analyzing the performance of a system. A system is said to be stable, for a particular interval of time, if the response, or output, of the system remains finite when it is excited by a set of finite inputs over the same time interval. In order to test a particular system model for stability, several testing criteria are available, depending on the nature and characteristics of the model. For LTI systems, the Nyquist stability and Routh's stability criterions are usually used. For nonlinear and time-varying systems, such stability criteria do not apply [49]. Lyapunov stability analysis is the most common method for the stability determination of non-LTI systems [50].

A system is said to be unstable if, for a particular range of operations, the output tends to infinity for any one, or combination, of its input excitations. Mathematically, the stability of a system, $G(t)$, can be defined as Equations (1) and (2).

$$\forall t \in [t_0, \infty)$$

If

$$\lim_{t \rightarrow \infty} \|G(t)\| = \infty, \quad (1)$$

then, $G(t)$ is unstable for every value of time, t .

Moreover, if

$$\lim_{t \rightarrow \infty} \|G(t)\| = K \quad (2)$$

where ' K ' is the finite value, then, $G(t)$ is stable for every value of time, t , where t_0 = initial time.

For state-space systems, there are different concepts of stability, such as uniform stability (a more general way of defining stability), asymptotic stability (eigen values of the system matrix have negative real parts), and exponential stability (system response decaying exponentially towards zero as time approaches infinity). There are applications where a system can possess uniform asymptotic stability, depending upon the equilibrium and the zero-state point of the state-space system.

2.2. Controllability

Controllability exhibits the structural features of a dynamic system and is a characteristic property. The conditions on the controllability and stability often govern the control solution. For a state-space control system, rules exist for the conduct of controllability tests. An LTI system is described by Equations (3) and (4).

$$\dot{x}(t) = A_{n \times n}x(t) + b_{n \times 1}u(t) \quad (3)$$

$$y(t) = c_{1 \times n}x(t) + d_{1 \times 1}u(t) \quad (4)$$

where

A = System coefficient matrix

b = Input coefficient matrix

c = Output coefficient matrix

d = Input-output coupling matrix

A system defined by Equations (3) and (4) is said to be controllable if there exists an input, $u_{[0, t_1]}$, that enables the system to be transferred from an initial state, $x(0) \triangleq x^0$, to another state, x^1 , in a finite interval of time, $\Delta t = t_1$. A system is said to be completely controllable if all of its initial states are controllable; otherwise, the system is said to be uncontrollable.

The solution of Equation (3) is:

$$x(t) = e^{At}x^0 + \int_0^t e^{A(t-\tau)}bu(\tau)d\tau \quad (5)$$

assuming, without loss of generality, that $x^1 \equiv 0$, the system is controllable if:

$$\begin{aligned} & \forall u_{[0,t_1]} \text{ input,} \\ & -x^0 = \int_0^{t_1} e^{At}bu(\tau)d\tau \end{aligned} \quad (6)$$

where τ = Time variable.

From Equation (6), it can be observed that a system's complete controllability depends on A and b and is independent of c and d . Equation (5) represents the system controllability of the pair (A, b) . As per Equations (3)–(6), no constraint is imposed on the inputs or on the trajectory that the state should follow. This implies that a system could be controllable for a finite interval of time even if it is uncontrollable. Such a restriction does not enable the control plant to follow the control rules for a desired interval of time. However, if the system satisfies the controllability condition, then there can be no intrinsic limitation on the design of the control system for the plant. If the processing and the significant variables of the system model are maintained within the acceptable range, then it is immaterial whether the plant is completely controllable or not.

Practically, building energy systems are nonlinear in nature and small perturbations of A and b can cause an uncontrollable system to become controllable. For MIMO systems, a plant can achieve complete controllability if the number of control variables is increased. Moreover, for models with redundant state variables, an increase in the number of control variables can cause a controllable system to become uncontrollable. For a MIMO system, such as a building energy system, it is usually difficult to compute system controllability using Equation (6).

2.3. Realizing Stability through Root Locus Plots

The frequencies at which the system under study tends to reach towards infinity are regarded as poles, and the frequencies at which the system tends to reach towards the origin, or zero, are regarded as zeros of the system. The transfer function representation of a particular system helps in assessing its stability without having to solve the differential equation characterizing the system. For a linear system to be stable, all the poles of the transfer function must possess negative real parts, i.e., their position should be within the left half of the s -plane. The performance of a particular system can be analyzed using the pole-zero plot or the root-locus plot. For a linear system, if the number of poles is greater than that of zeros, then that system is said to be a practically realizable system [36].

For a closed-loop MIMO system, such as a building energy system, the basic characteristic of the response is analyzed using the location of the closed-loop poles. Under situations of variable gain for the building energy system, the value of the gain at any instant in time depends on the position of the poles. It is, therefore, important to have knowledge of the trajectory of the closed-loop poles, as the gain is varied over the simulation period in the s -plane. If the position of the poles remains the same after varying the gain value, then a compensator has to be added to achieve the desired results. The root-locus plots the roots of the characteristic equation for all values of a system parameter. A block diagram of a building energy system with a controller is shown in Figure 2.

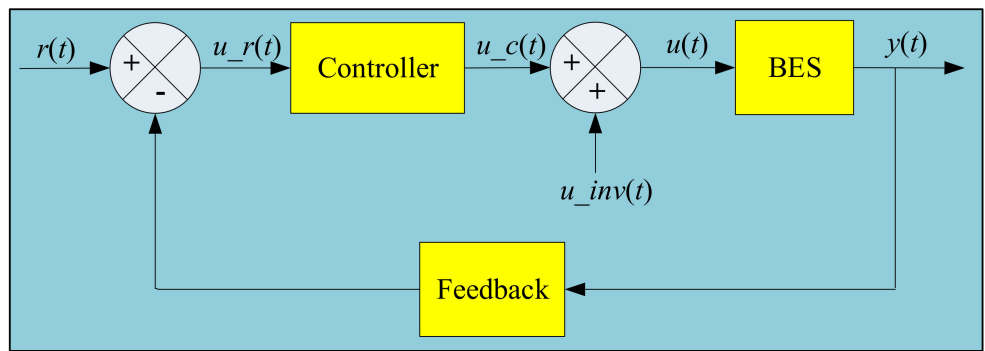


Figure 2. Block diagram for controller-fed building energy system (BES) under study.

The closed-loop transfer function for the system shown in Figure 2 is given as Equation (7).

$$\frac{Y(s)}{R(s)} = \frac{G_C(s)G_{BES}(s)}{1 + G_C(s)G_{BES}(s)H(s)} \quad (7)$$

where

$Y(s)$ = Laplace transform of actual output of the system, $y(t)$

$R(s)$ = Laplace transform of input signal, $r(t)$

$G_C(s)$ = System transfer function of controller with $u_r(t)$ as input and $u_c(t)$ as output

$G_{BES}(s)$ = Building energy system's transfer function under study with $u(t)$ as input and $y(t)$ as output

$H(s)$ = Negative feedback signal

$r(t)$ = Desired output

$u_{inv}(t)$ = Dynamic inverse input and is defined as per the IDIT, given as Equation (8)

$$L[u_{inv}(t)] = U_{inv}(s) = \begin{bmatrix} -(CB)^{-1} & CAx(s) - (CB)^{-1} & C \end{bmatrix} \quad (8)$$

The characteristic equation of the system is given as Equation (9):

$$1 + G_C(s)G_{BES}(s)H(s) = 0 \quad (9)$$

$$G_C(s)G_{BES}(s)H(s) = -1 \quad (10)$$

by using the equality of angles and magnitudes for complex numbers,

$$\angle G_C(s)G_{BES}(s)H(s) = \pm 180^0(2n + 1) \quad (11)$$

where

$n = 0, 1, 2, \dots$

and,

$$|G_C(s)G_{BES}(s)H(s)| = 1 \quad (12)$$

Equations (11) and (12) are called the angle and magnitude conditions, respectively. The closed-loop poles of the building energy system can be computed by evaluating s from the abovementioned equations. The locus of all such s -points in the complex s -plane is called the root locus.

3. Stability and Controllability Analysis of Building Energy Systems

After estimating and identifying the parameters of the building energy system model, it is crucial to analyze the performance of the model. Before developing the control strategies for building energy systems, it is imperative to conduct feasibility studies and tests on the building energy system model in order to set performance standards for model selection and evaluation. The set of the input and output parameters of energy systems used for the stability analysis and controllability assessment are shown in Figure 3.

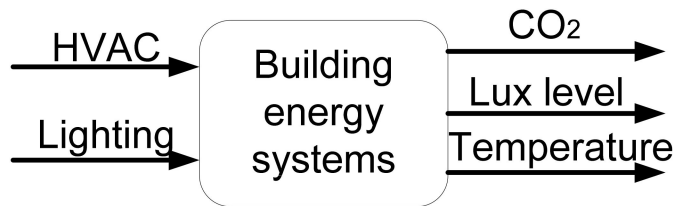


Figure 3. Building energy system model.

The primary aim of the developed HVAC system model is to regulate the building space air temperature and CO₂ concentration. This is to ensure the optimal air temperature for the comfort of the occupants, and the effective circulation of fresh air in and out of the building space. The outputs of an HVAC system, which are T_{BS} and RH_{BS} , are considered for the controllability analysis. A process flowchart of the strategy for the stability and controllability assessments followed in the present study is shown in Figure 4. In the present study, the potential of the developed building energy system to be stabilized for the development of any energy control strategy is investigated by using the IDIT, which was developed for the aerospace industry [31,47].

The building energy system model developed in [23,26] is represented in state-space form as Equations (13) and (14):

$$\dot{X} = AX + BU \quad (13)$$

$$Y = CX + DU \quad (14)$$

where

\dot{X} = Vector matrix of first-order derivatives of building energy system temperatures

X = Nodal temperature state-matrix

U = Building energy system's temperature and HVAC load parameter vector

Y = Vector of T_{BS} , building space temperature and RH_{BS} , building space relative humidity

A = Building energy system model coefficient matrix

B = Vector matrix of building energy system model input coefficients

C = Vector matrix of output coefficients

D = Coupling matrix of input and output coefficients

The parameters of building energy system models operate simultaneously in a designed control algorithm, and each parameter acts on an actuator to reach a desired setpoint value/level. The building energy system state-space model, as given in Equations (13) and (14), is converted into transfer function form as Equations (15)–(18):

$$G(s) = C(sI - A)^{-1}B + D \quad (15)$$

$$= \frac{C[\text{adj}(sI - A)]B}{|sI - A|} + D \quad (16)$$

$$= \frac{C[\text{adj}(sI - A)]B + D|sI - A|}{|sI - A|} \quad (17)$$

$$= \frac{N_{P-Z}(s)}{D_{P-Z}(s)} \quad (18)$$

where

N_{P-Z} = Numerator polynomial of $G(s)$ after pole-zero cancellation

D_{P-Z} = Denominator polynomial of $G(s)$ after pole-zero cancellation.

The poles of $G(s)$ are the roots of $D_{P-Z}(s)$, which are the uncancelled eigen values of A (substituting λ for s), as in Equations (19) and (20):

$$D_{P-Z}(s) = |sI - A| = 0 \quad (19)$$

and,

$$|\lambda I - A| = 0 \quad (20)$$

Equation (20) provides the internal system poles and, as there are pole-zero cancellations in computing $G(s)$, Equation (20) provides the information on the input/output (external) stability of the system. Thus, for internal stability, all the eigen values of A must have negative real parts.

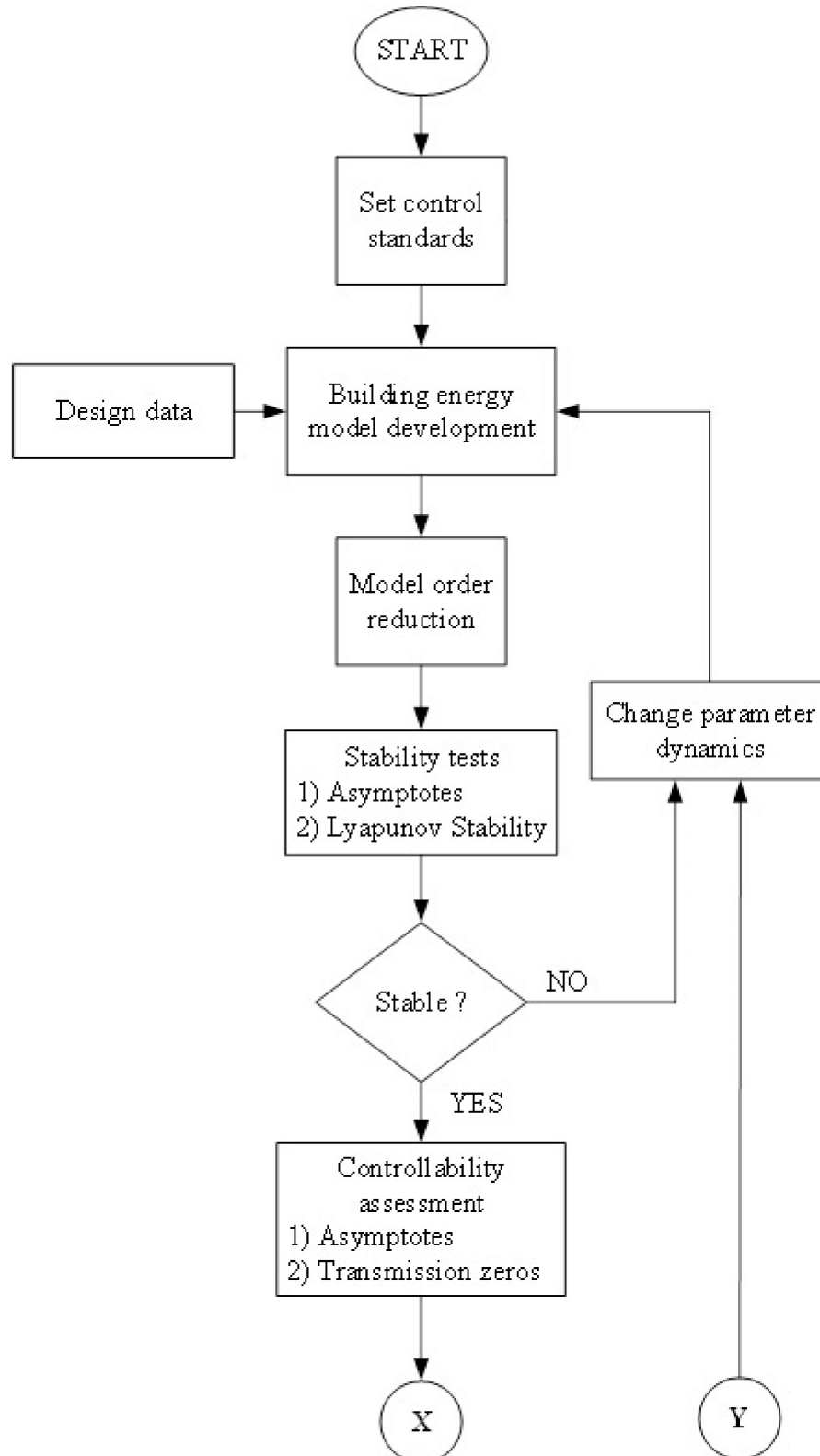


Figure 4. *Cont.*

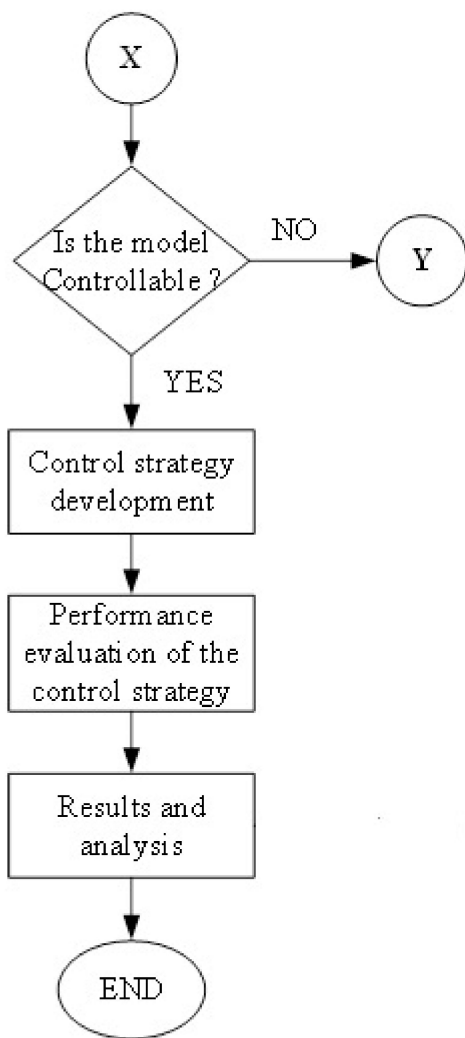


Figure 4. Developed process flowchart for building energy system stability and controllability assessment.

Transmission Zeros

For a linear-time-invariant system, state equations, representing a system, are equal in number to that of closed-loop poles. Transmission zeros are the states corresponding to the infinite poles of the system under study. Such poles are the asymptotes, or branches of the root loci, describing the system. The present study involves the control of the building space air temperature, relative humidity, CO₂ concentration, and lux level, and these parameters will be fed back into the system, i.e., the output of the feedback block of Figure 2.

The inverse dynamics input, $u_{inv}(t)$, enables the system poles to be positioned on top of system zeros, thereby making the states of the system controllable. This means that the closed-loop poles of the system are nothing but the open-loop zeros of the same system. The zeros are determined by the open-loop transfer function, given as Equation (21).

$$G(s) = \frac{CB}{s} \quad (21)$$

The transmission zeros for a model are determined by equating Equations (13) and (14) to zero, i.e.,

$$(A - sI)X(s) + BU(s) = 0 \quad (22)$$

$$CX(s) + DU(s) = 0 \quad (23)$$

Equations (22) and (23) are written in matrix form as Equation (24).

$$\begin{bmatrix} A - sI & B \\ C & D \end{bmatrix} \begin{bmatrix} X(s) \\ U(s) \end{bmatrix} = 0 \quad (24)$$

The transmission zeros can then be finally determined by calculating the determinant of Equation (24):

$$\begin{vmatrix} A - sI & B \\ C & D \end{vmatrix} = 0 \quad (25)$$

4. Stability Analysis of Building Envelope Model

The state-space stability of the building envelope model is analyzed by observing the eigen values of the coefficient matrix, A . The coefficient matrix for the building envelope, shown in Figure 3, are given as Equations (26)–(30). The coefficient matrix for the outdoor wall is given as Equation (26):

$$A_{OW} = \begin{bmatrix} -0.239 & 0.0478 \\ 0.008435 & -0.01518 \end{bmatrix} \quad (26)$$

where A_{OW} = the coefficient matrix for the outdoor wall state-space model of a building energy system.

A pole-zero plot for Equation (26) is shown as Figure 5.

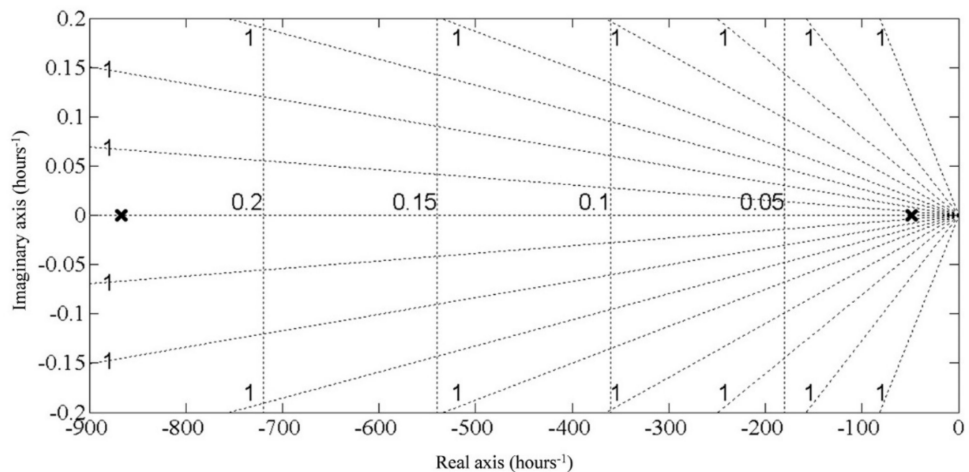


Figure 5. Pole zero plot for outdoor wall of the building energy system.

There are two poles for the outdoor wall model, as A_{OW} is of a two-by-two dimension. The poles of the outdoor wall state-space model are at -0.2408 and -0.0134. The poles of the outdoor wall state-space model lie on the left half of the pole-zero plane and, thus, the model is stable. Similarly, the coefficient matrices of the adjacent wall, roof, floor, and lobby wall are given as Equations (27)–(30), and the corresponding pole-zero plots are given as Figures 6–9, respectively.

$$A_{adjw} = \begin{bmatrix} -1.967 & 0.3934 \\ 0.06942 & -0.125 \end{bmatrix} \quad (27)$$

where A_{adjw} = Coefficient matrix for adjacent wall building envelope model.

$$A_{roof} = \begin{bmatrix} -0.8096 & 0.1619 \\ 0.02858 & -0.05144 \end{bmatrix} \quad (28)$$

where A_{roof} = Coefficient matrix for roof wall building envelope model.

$$A_{floor} = \begin{bmatrix} -1.115 & 0.223 \\ 0.03936 & -0.07085 \end{bmatrix} \quad (29)$$

where A_{floor} = Coefficient matrix for floor wall building envelope model.

$$A_{lobby} = \begin{bmatrix} -0.897 & 0.2951 \\ 0.07452 & -0.0525 \end{bmatrix} \quad (30)$$

where A_{lobby} = Coefficient matrix for lobby wall building envelope model.

The poles of the adjacent wall state-space model are at -1.9816 , and -0.1102 , whereas the poles of the roof state-space model are at -0.8157 , and -0.0454 .

The poles of the floor state-space model are at -1.1235 , and -0.0625 , whereas the poles of the lobby wall state-space model are at -0.9223 , and -0.0272 . Every pole of the system transfer functions for the construction elements lie in the negative half of the s-plane. This shows that the building envelope model is stable. Moreover, because of the absence of any pole-pairs on the s-plane, the system is completely stable and does not oscillate.

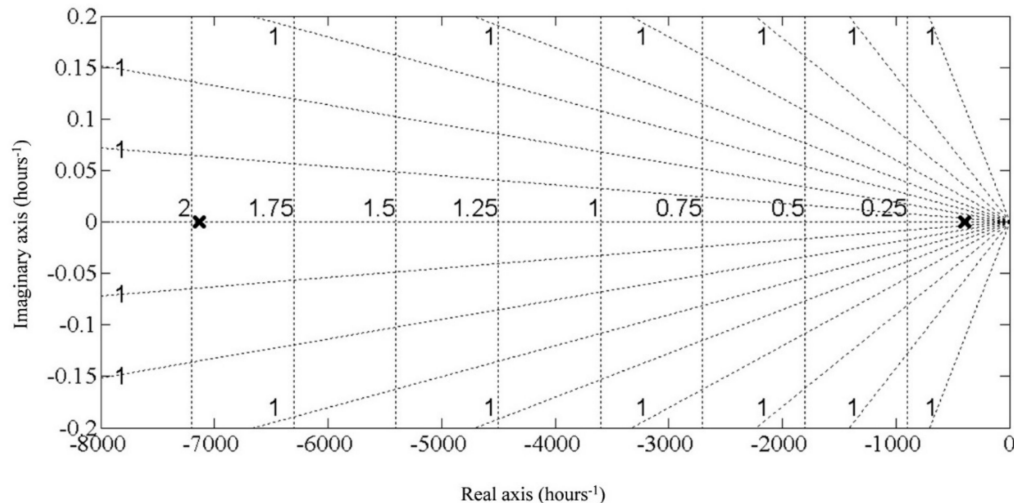


Figure 6. Poles location for adjacent wall model of the building energy system.

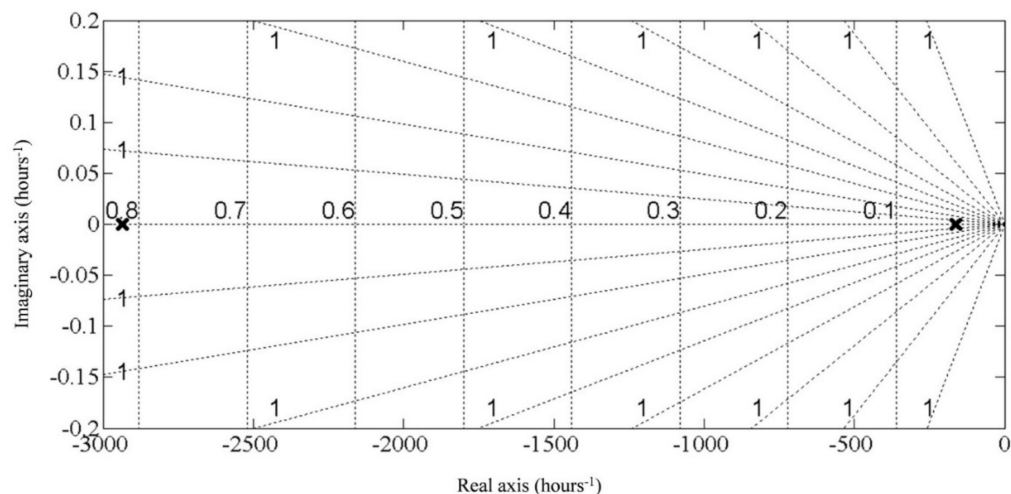


Figure 7. Poles location for roof wall model of the building energy system.

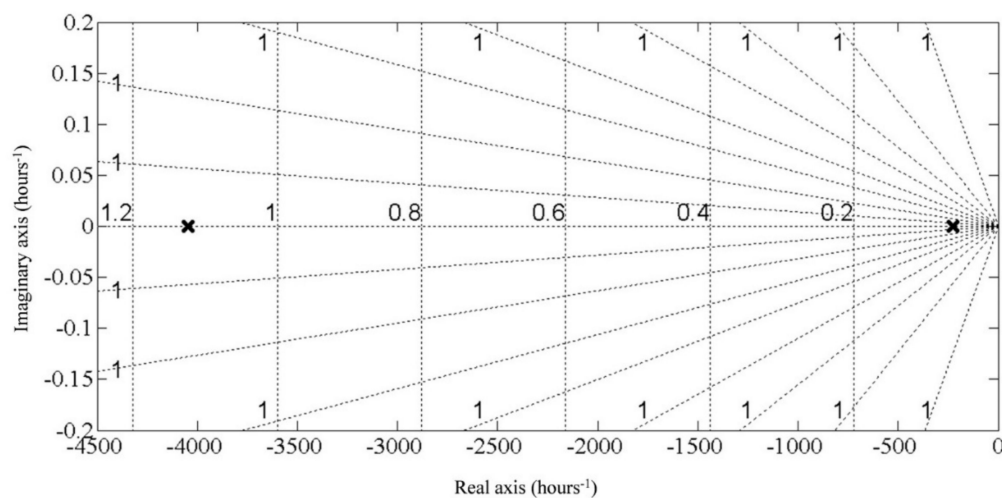


Figure 8. Poles location for floor wall model of the building energy system.

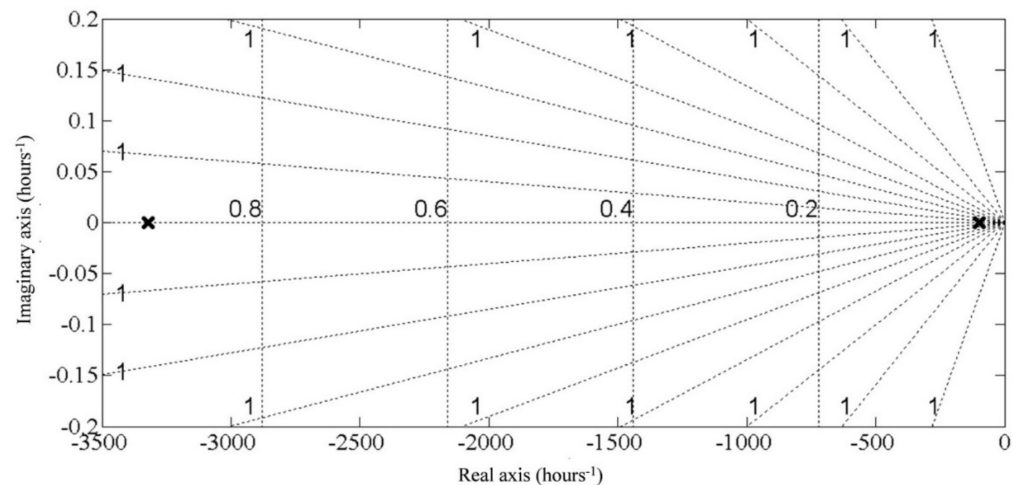


Figure 9. Poles location for lobby wall model of the building energy system.

The coefficient matrix for the window state-space model is given as Equation (31):

$$A_{win} = \begin{bmatrix} -0.1871 & 0.1003 \\ 0.010005 & -0.0986 \end{bmatrix} \quad (31)$$

where A_{win} = Coefficient matrix for window state-space model of building energy system.

The pole-zero plot for the window state-space model, described as per Equation (31), is shown in Figure 10.

There are two poles for the window model, as A_{win} is of a two-by-two dimension. The poles of the window state-space model lie on the left half of the pole-zero plane. The poles of the window state-space model are at -0.0884 and -0.1973 . The position of these poles makes the window state-space model stable.

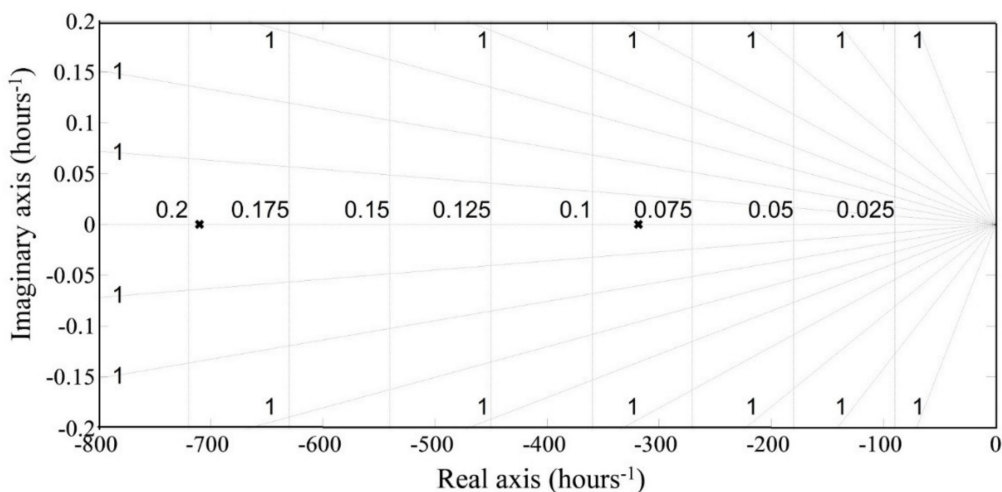


Figure 10. Pole-zero plot for window of the building energy system.

5. Stability Analysis of Building Space Model

The state-space stability of the building space model is analyzed by observing the eigen values of the coefficient matrix, A . The coefficient matrix for the building space state-space model, (A_{BS}), is given as Equation (32).

$$A_{BS} = \begin{bmatrix} -6.65 \times 10^{-3} & 6.32 \times 10^{-3} & 0 & 0 \\ 2.99 \times 10^{-5} & -3.23 \times 10^{-5} & 2.43 \times 10^{-6} & 0 \\ 0 & 9.15 \times 10^{-5} & -1.9 \times 10^{-4} & 9.89 \times 10^{-5} \\ 0 & 0 & 2.98 \times 10^{-6} & -5.35 \times 10^{-5} \end{bmatrix} \quad (32)$$

Using the eigen values of Equation (32) and the A_{BS} of the building space model, then poles location is shown in Figure 11.

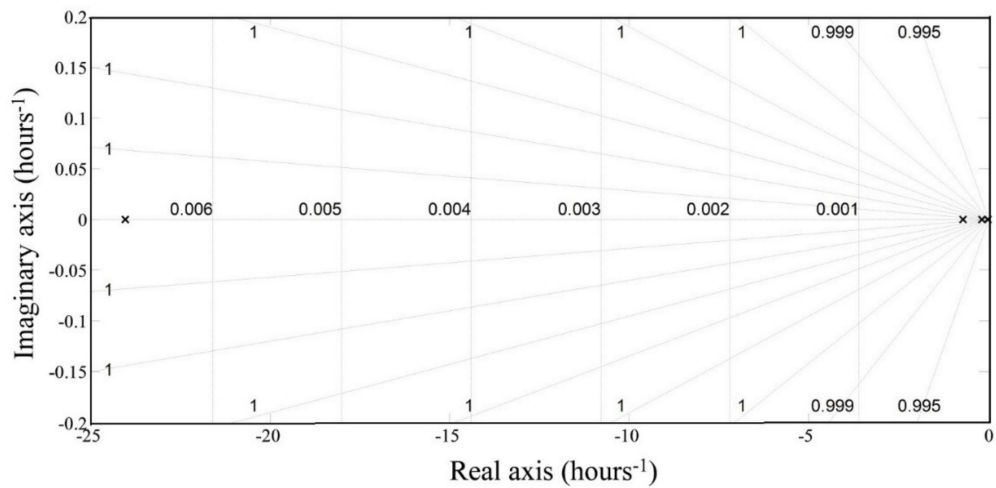


Figure 11. Poles location for building space model of the building energy system.

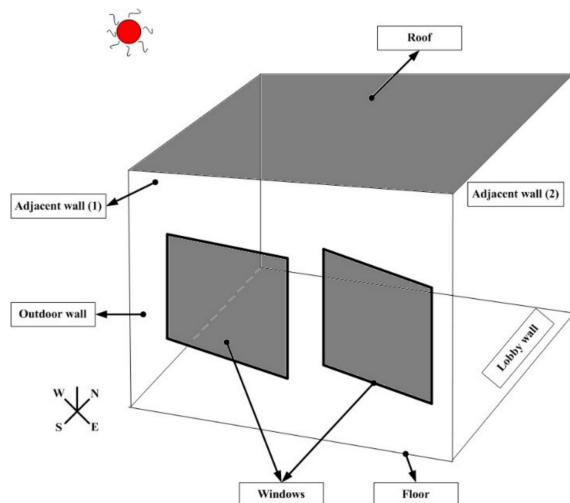
There are four poles for the building space model, as A_{BS} is of a four-by-four dimension. The poles of the building space model are at -0 , -0.0001 , -0.0002 , and -0.0067 . The poles of the building space model lie on the origin and on the left half of the pole-zero plane. There are three poles very close to the origin. These poles tend to make the building space model marginally stable.

6. Stability Analysis and Controllability Assessment of Building Space Model

A typical HVAC system is responsible for both the temperature and humidity control of the building space. With consideration given to all the building elements responsible for hygrothermal energy transfer processes within a building space, a full-order building energy system model has been developed.

6.1. Building Energy System Model

A virtual test setup was developed in MATLAB/Simulink and a thermal resistor-capacitor network was used for the building energy system model representation. A schematic of the test setup is shown in Figure 12. The parameter values of the test setup are given in Appendix A.



Building element	Orientation
Adjacent wall(1)	West
Outdoor wall	South
Lobby wall	East
adjacent wall(2)	North

Figure 12. Schematic of the test setup for building energy system model.

In order to assess the complete stability and controllability of the building energy system, energy transfer equations governing the development of the model have been reproduced as Equation (33):

$$\rho_a V_a C_{pa} \frac{dT_{BS}}{dt} = \dot{Q}_{cas} + \dot{Q}_{struct} + \dot{Q}_{vent} + \dot{Q}_{therm} \quad (33)$$

where

\dot{Q}_{cas} = Rate of heat transfer due to causal factors of solar radiation, lighting, occupancy, and appliances in the building space/zone, W/m^2

\dot{Q}_{struct} = Rate of heat transfer due to structural elements of the building space, such as windows, etc., W/m^2

\dot{Q}_{vent} = Rate of heat transfer due to ventilation and/or circulation of air within the building space, W/m^2

\dot{Q}_{therm} = Heat transfer rate of heating/cooling from the plant, W/m^2

ρ_a = Density of air in the building space, kg/m^3

V_a = Specific volume of air in the building space, m^3/kg

C_{pa} = Specific heat capacity of air in the building space, kJ/kg-K

The rate of heat transfer due to causal factors is given as Equation (34):

$$\dot{Q}_{cas} = \dot{Q}_{sol} + \dot{Q}_L + \dot{Q}_{occ} + \dot{Q}_{appl} \quad (34)$$

where \dot{Q}_{sol} = Rate of heat transfer due to solar radiation through windows, W/m^2 and is given by Equation (35):

$$\dot{Q}_{sol} = \alpha_a \sigma_s A_{win} H_{sol} \quad (35)$$

where

α_a = Absorptivity constant

σ_s = Transmissivity of the window

A_{win} = Effective surface area of window, m^2

H_{sol} = Solar radiation incident on the window surface, W/m^2

and,

\dot{Q}_L = Amount of power converted into heat due to lighting luminaires installed in the building space, W/m^2 , and is given by Equation (36):

$$\dot{Q}_L = k_e P_L \quad (36)$$

where

k_e = Proportion of lighting power contributing to the heat gains

P_L = Wattage rating of the luminaires, W

and,

\dot{Q}_{occ} = Heat transfer rate due to occupants of the building space, W/m^2 , and is given by Equation (37):

$$\dot{Q}_{occ} = n_{occ} P_{occ} \quad (37)$$

where

n_{occ} = Number of occupants

P_{occ} = Occupants heat gain rate (calculated as per ASHRAE principles), W ,

and,

\dot{Q}_{appl} = Heat transfer due to appliances, such as computers/desktops, laptops, and other peripherals operating in the building space, W/m^2 , and is given by Equation (38):

$$\dot{Q}_{appl} = \dot{Q}_{laptops} + \dot{Q}_{desktops} + \dot{Q}_{peripherals} = \sum n_{appl} P_{appl} \quad (38)$$

where

n_{appl} = Number of appliances operating within the building space

P_{appl} = Heat gain produced by the appliances (calculated as per ASHRAE principles), W .

The rate of heat transfer ventilation and the circulation of air within the building space is given as Equation (39):

$$\dot{Q}_{vent} = \dot{Q}_{int} + \dot{Q}_{ext} + \dot{Q}_{inf} + \dot{Q}_{mech} \quad (39)$$

where

\dot{Q}_{int} = Air change due to internal thermal forces, W/m^2 , and is given by Equation (40):

$$\dot{Q}_{int} = V_a \eta_t \rho_a C_{pa} (T_{out} - T_{BS}) \quad (40)$$

and

\dot{Q}_{ext} = Air change due to external thermal forces, W/m^2 , and is given by Equation (41).

$$\dot{Q}_{ext} = V_a \eta_v \rho_a C_{pa} (T_{out} - T_{BS}) \quad (41)$$

and

\dot{Q}_{inf} = Air change due to infiltration through the building space, W/m^2 , and is given by Equation (42).

$$\dot{Q}_{\text{inf}} = V_a \eta_i \rho_a C_{p_a} (T_{out} - T_{BS}) \quad (42)$$

and

\dot{Q}_{mech} = Air change due to forced/mechanical ventilation through the building space, W/m^2 , and is given by Equation (43).

$$\dot{Q}_{\text{mech}} = q_{\text{mech}} \rho_a (T_{BS} - T_{out}) \quad (43)$$

The differential equation for the amount of water vapor in the air of the building space is given as Equation (44).

$$\rho_a V_a \frac{dw_{BS}(t)}{dt} = W_{\text{int}} - W_{\text{therm}} - W_{\text{wind}} - W_{\text{nat}} - W_{\text{mech}} \quad (44)$$

where

w_{BS} = Building space humidity gain, kg/s

W_{int} = Internal humidity gain, kg/s

W_{therm} = Loss of humidity due to thermal buoyancy, kg/s , and is given as Equation (45).

$$W_{\text{therm}} = V_a \eta_v \rho_a (w_{BS} - w_{out}) \quad (45)$$

and

W_{wind} = Humidity loss by wind pressure, kg/s and is given by Equation (46).

$$W_{\text{wind}} = V_a \eta_w \rho_a (w_{BS} - w_{out}) \quad (46)$$

and

W_{nat} = Humidity loss by natural air change rate, kg/s and is given by Equation (47).

$$W_{\text{nat}} = V_a \eta_i \rho_a (w_{BS} - w_{out}) \quad (47)$$

and

W_{mech} = Humidity loss by mechanical/forced ventilation, kg/s and is given by Equation (48).

$$W_{\text{mech}} = q_{\text{mech}} \rho_a (w_{BS} - w_{out}) \quad (48)$$

Equations (34)–(49) of the building energy system are represented linearly in a matrix form as Equations (49) and (50).

$$\dot{X} = AX + BU + fD \quad (49)$$

$$Y = CX \quad (50)$$

where D = Vector of disturbances.

Small amplitude perturbation is studied by analyzing the dynamic behavior of the building energy system under study using the state-space model of Equation (49) and Equation (50). It is to be noted that these equations represent a steady-state equilibrium condition. A , B , C , and f represent the time-invariant matrices of the constants. The state vectors of the complete building energy system model under study are given as Equations (51)–(53).

$$X = [T_{BS} \quad T_{BCE} \quad T_{\text{int}} \quad W_{BS}]^T \quad (51)$$

$$U = [\dot{Q}_{\text{HVAC}} \quad T_{\text{vent}}]^T \quad (52)$$

$$D = [H_{\text{sol-rad}} \quad v_{\text{wind}} \quad W_{out} \quad Q_{\text{Cas}} \quad W_{BS} \quad Q_{\text{Light}}]^T \quad (53)$$

The stability and controllability of the system were assessed using the *CB* matrix and IDIT [32]. The *CB* stability matrix of the system is given as Equation (54) and simplified as Equation (55).

$$CB = \begin{bmatrix} \frac{\beta}{\rho_a V_a C_{pa}} & \frac{(T_{out} - T_{BS})}{V_a} \\ 0 & \frac{(W_{BS} - W_{out})}{V_a} \end{bmatrix} \quad (54)$$

$$CB = \begin{bmatrix} b_{11} & b_{12} \\ b_{21} & b_{22} \end{bmatrix} \quad (55)$$

From the equation, it can be observed that there exists a cross-coupling between temperature and humidity. This is achieved because of mechanical ventilation, (b_{12}), which affects both the humidity and the temperature values of the building space. The primary cause for this cross-coupling is due to water evaporation in the building space, which adds to the hygrothermal losses. Such losses, however, are difficult to quantify and are modeled as disturbances to the developed building energy system model.

Term b_{12} of the *CB* matrix represents a cross-coupling of the temperature parameter that, in the present study, is equal to the difference in the building space and outdoor temperatures. The magnitude of the b_{12} parameter changes with seasonal variations. Smaller differences in the building space and outdoor temperature yield smaller b_{12} values, which represent the summer seasonal condition. This means that the developed building energy system model can employ a conventional PID-controlled HVAC system. During winter conditions, the temperature difference will be large and, hence, b_{12} will be a larger value. Such scenarios will demand the modeling of an external parameter for the mechanical ventilation of the PID-controlled HVAC system.

6.2. Simulation Results

In the present study, the developed building energy system is a multi-input multi-output system. Asymptotes for such a system can be represented using the *CB* matrix's eigen values. The asymptotes for the developed building energy system model are given as Equation (56).

$$|sA_I + g(CB)\sigma| = 0 \quad (56)$$

where

g = Gain value which can be regulated globally throughout the system

σ = Scalar gain value.

Equations (55) and (56) can be combined as follows:

$$|sI + g(CB)\sigma| = \begin{vmatrix} s_1 + gb_{11}\sigma_1 & gb_{12} \\ 0 & s_2 + gb_{22}\sigma_2 \end{vmatrix} \quad (57)$$

$$\Rightarrow \begin{vmatrix} s_1 + gb_{11}\sigma_1 & gb_{12} \\ 0 & s_2 + gb_{22}\sigma_2 \end{vmatrix} = 0 \quad (58)$$

$$(s_1 + gb_{11}\sigma_1)(s_2 + gb_{22}\sigma_2) = 0 \quad (59)$$

$$s_1 = -gb_{11}\sigma_1, \quad s_2 = -gb_{22}\sigma_2 \quad (60)$$

The above equation yields the values of s -, which are the asymptotes of the building energy system model's output parameters, viz., the building space temperature and humidity, which can be expressed as follows:

$$s_1 = -g_{0 \rightarrow \infty} \frac{\beta}{\rho_a V_a C_{pa}} \sigma_1 \quad (61)$$

$$s_2 = -g_{0 \rightarrow \infty} \frac{(W_{out} - W_{BS})}{V_a} \sigma_2 \quad (62)$$

where s_1 represents the asymptote for the building space air temperature, and the negative sign indicates that the transient response of the temperature will be stable and there will not be any oscillations in the temperature parameter to reach its steady-state value, whereas s_2 becomes positive under unconditioned situations where the building space humidity levels are greater than that of the outdoor level. Under such instances, the transient humidity response becomes unstable as well as uncontrollable, as s_2 aligns to the positive of the s -plane. This is occurring because of the term, b_{22} , of the CB matrix. In order to make the transient humidity response stable and controllable, the s_2 asymptote needs to be realigned. This can be achieved by allotting a negative value to the gain, σ_2 . This condition is shown in the s -plane and is given in Figure 13.

The asymptotes of Figure 13 are the function of the temperature and humidity differences between the outdoor environment and the building space. Moreover, as the asymptotes are not at an angle, with respect to the real axis, and are negatively aligned towards the left half of the plane, the variation in the operating temperature and humidity levels will not affect the controllability of the developed building energy system model. If we consider the region to the right of the imaginary axis, the response can be seen to be increasing as the time increases. That means that no defined final state of the building energy system can be reached as time, $t \rightarrow \infty$.

By considering all of the asymptotes for all of the parameters in the developed building energy system model, total stability can be assessed using the TZ matrix of an MIMO system. The TZ matrix represents the transmission zeros of an MIMO system and is given as Equation (63).

$$TZ = \begin{vmatrix} a_{11} - s_1 & a_{12} & a_{13} & 0 & b_{11} & b_{12} \\ a_{21} & a_{22} - s_2 & 0 & 0 & 0 & 0 \\ a_{31} & 0 & a_{33} - s_3 & 0 & 0 & 0 \\ 0 & 0 & 0 & a_{44} - s_4 & 0 & b_{42} \\ c_{11} & 0 & 0 & 0 & 0 & 0 \\ 0 & 0 & 0 & c_{24} & 0 & 0 \end{vmatrix} = 0 \quad (63)$$

On performing reductions, the TZ matrix is remodified as Equation (64).

$$TZ = \det \begin{vmatrix} a_{22} - s_2 & 0 \\ 0 & a_{33} - s_3 \end{vmatrix} = 0 \quad (64)$$

The transmission zeros computed by solving the determinant of Equation (64) are given as Equation (65).

$$(a_{22} - s_2)(a_{33} - s_3) = 0 \quad (65)$$

The transmission zeros are given as Equations (66) and (67).

$$s_2 = a_{22} = \frac{-2A_w(U_{wo} + U_{wi})}{\rho_w V_w C_{p_w}} \quad (66)$$

$$s_3 = a_{33} = \frac{-2A_m U_m}{\rho_m V_m C_{p_m}} \quad (67)$$

From the above equations, it can be seen that s_2 and s_3 are negatively aligned on an s -plane, thereby signifying the total stability of the developed building energy system model. As is evident from Equations (66) and (67), the transmission zeros are independent of outdoor environmental variations, such as temperature, humidity, and solar radiation. The transmission zeros vary with the variations in the thermophysical properties of the building construction elements and the thermal transmittance of the internal and external thermal mass of the building space.

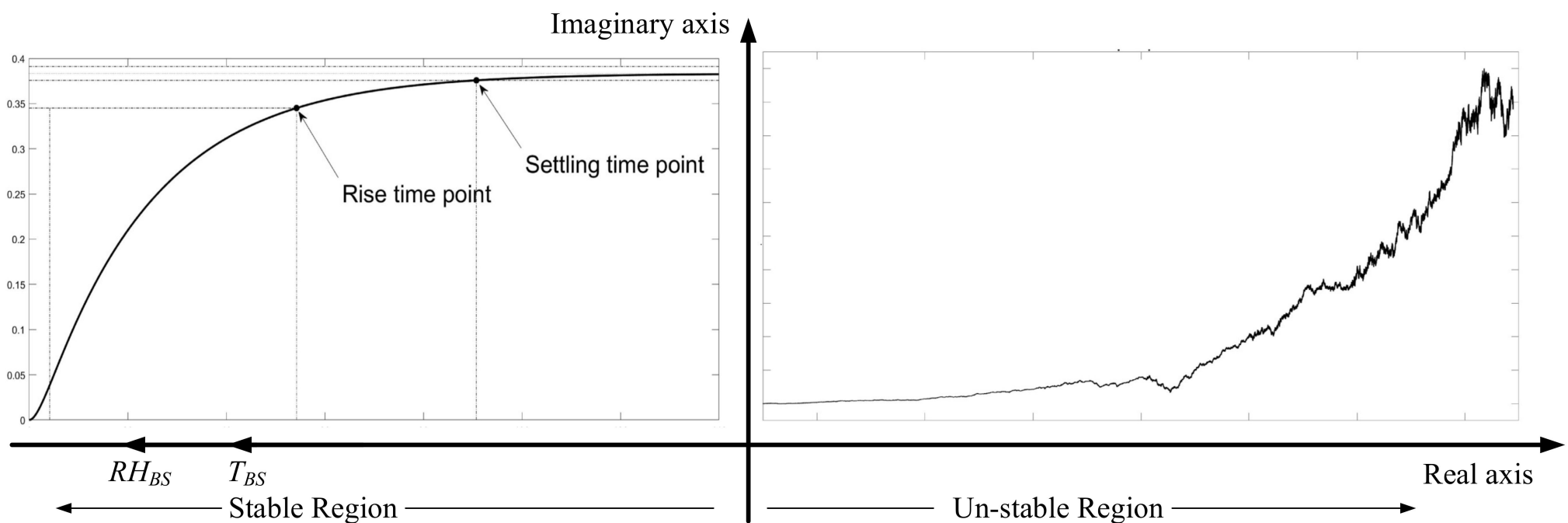


Figure 13. Asymptote for the building space air humidity and temperature control.

7. Discussion and Limitations of the Present Study

The control strategies developed for building energy systems become unstable for a particular range of operations when the system is simulated for a longer period of time, resulting in occupant discomfort and high-energy consumption. The present study applies conventional stability tests on the developed building energy system model and assesses the state-control trajectory of the model against the parameters of the building space air temperature, relative humidity, lux level, and CO₂ concentration.

The methodology for conducting the stability and controllability assessment tests on the building energy model is presented. The developed testing methodology assists in determining the feasibility of an energy control strategy that can be applied in order to enhance the energy performance of a building. The state-space building energy system enables the representation of the interactions between the building space variables (both outdoor and indoor), such as air temperature, humidity, occupancy, and other causal thermal gains and state variables, such as the nodal temperatures of the building elements, HVAC heating/cooling load, and the lighting system load. Gaining knowledge about such interactions enables the modeler to determine the extent to which state trajectories can be controlled by varying the input parameters to the building energy system.

The thermal transmittance of the multilayered construction elements is reciprocal of the corresponding R-value. For lower costs and lower emissions, the U-value is kept low, adhering to the building regulations and codes. Applying this to the developed building energy system model yields low-thermal-capacity multilayered construction elements making up the building space. This increases the reaction speed to the control inputs as the location of zero is a function of the heat transmitted through the fabric and the heat stored in it. Thus, the thermal capacity of the construction element is significant for responsive control.

The present study does not consider the seasonal variations on the building energy system model. The controllability assessment approach presented in this paper may need modification when applied to climate-adaptive building energy systems. However, the approach for conducting the stability tests may remain identical. Passive heating and cooling strategies need to be explored and included, and the air gaps in the multilayered construction elements have been ignored.

The present study did not consider the effects of thermal bridging in the building walls. In order to develop a model with improved sophistication, the effective thermal transmittance of the building envelope can be calculated using available methods, such as ASTM Standard C1363, the effective area approach, the weighted average method, and thermographic survey. An accurate thermal model needs to be considered in order to make the assessment approach widely applicable. The present study does not demonstrate a controllability assessment for other parametric outputs, such as heating/cooling power, lighting load, energy usage, etc.

8. Conclusions

Because of the presence of one stable transmission zero during building space air temperature control (without humidity control), conventional single-input single-output (SISO) controllers, such as the PI controller, are adequate for controlling the building space air temperature without giving consideration to humidity. A stable and controllable building energy system model can now be used to develop control strategies for the effective management of the energy control and occupant comfort of buildings.

The discussions outlined above shall not always be true in the case of an unconditioned passive building. This is because the passive design of a building makes use of the thermal mass and capacity of the construction elements for satisfying the cooling load and also for thermal storage. Applying the current controllability assessment approach will yield sluggish and slow responses for the temperature and humidity parameters. However, this shall not be a concern, as the present study focuses primarily on conditioned building

energy system modeling, where the PID-controlled HVAC system exists for the humidity and temperature control of the building space.

Investigating the stability and controllability of building energy system models may also help in reducing the validation errors. Though the approach reported in this paper may be used for building energy system model verification, the determination as to what degree the developed model actually represents the physical real world can be explored in the future. The approaches and techniques used for the uncertainty analysis of system variables can be clubbed with the developed IDIT approach, and the results obtained from the same can be analyzed. Such an approach may strengthen the verification, validation, and uncertainty analysis of building energy system models. This, in turn, shall lead to savings of both time and money.

Author Contributions: Methodology, V.S.K.V.H.; conceptualization, V.S.K.V.H. and A.K.; analysis, V.S.K.V.H.; writing—original script, V.S.K.V.H.; supervision, A.K.; writing—editing, T.A. and P.B. All authors have read and agreed to the published version of the manuscript.

Funding: This research received no external funding.

Institutional Review Board Statement: Not applicable.

Informed Consent Statement: Not applicable.

Data Availability Statement: Not applicable.

Conflicts of Interest: The authors declare no conflict of interest.

Appendix A

Numerical values of the test-case setup are given in Table A1.

Table A1. Numerical values of the BES model parameters.

BES Model	Parameter Values
Building space/zonal characteristics	
Building envelope	Volume (m^3) 500 Outdoor wall area (m^2) 60 Outdoor wall thermal resistance ($\text{m}^2 \text{ }^\circ\text{C}/\text{W}$) 3.2560 Outdoor wall thermal capacitance ($\text{J}/\text{m}^2 \text{ }^\circ\text{C}$) 129,074 Adjacent wall area (m^2) 40 Adjacent wall thermal resistance ($\text{m}^2 \text{ }^\circ\text{C}/\text{W}$) 2.1128 Adjacent wall thermal capacitance ($\text{J}/\text{m}^2 \text{ }^\circ\text{C}$) 333,166 Roof/Floor area (m^2) 120 Roof/Floor thermal resistance ($\text{m}^2 \text{ }^\circ\text{C}/\text{W}$) 0.4192 Roof/Floor thermal capacitance ($\text{J}/\text{m}^2 \text{ }^\circ\text{C}$) 319,120 Lobby wall area (m^2) 35 Lobby wall thermal resistance ($\text{m}^2 \text{ }^\circ\text{C}/\text{W}$) 0.4017 Lobby wall thermal capacitance ($\text{J}/\text{m}^2 \text{ }^\circ\text{C}$) 170,772 Window area (m^2) 16 Window U-value ($\text{W}/\text{m}^2 \text{ }^\circ\text{C}$) 2.8 Glass/glazing area (m^2) 8 Glass transmissivity 75% Ground reflectance 25%
Occupancy schedule	Daily operating hours 8 Start hours 10.00 Weekly operating days 6
HVAC system	
Ventilation	Reference air changes per hour (h^{-1}) 0.6
Control valve	Designed mass flow rate (kg/s) 0.252
Heat exchanger	Heat transfer coefficient ($\text{W}/\text{m}^2 \text{ }^\circ\text{C}$) 32.2 Thermal capacitance of fluid & material ($\text{J}/\text{ }^\circ\text{C}$) 68,300

Table A1. *Cont.*

BES Model	Parameter Values
Lighting	
Type of luminaire	Pendant fluorescent 2440 mm type lamps
Number of lamps	8
Wattage of each lamp (W)	8
Special allowance factor (F_{SA})	0.85
Lighting use factor (F_{use})	1

References

- IEA 2019. World Energy Statistics and Balances 2019, International Energy Agency. Available online: www.iea.org/statistics (accessed on 20 December 2020).
- IEA 2019. Energy Technology Perspectives, Buildings Model. International Energy Agency. Available online: www.iea.org/buildings (accessed on 20 December 2020).
- Khan, M.A.; Mishra, S.; Harish, V.S.K.V. Grid connected energy efficient building with roof top SPV. In Proceedings of the International Conference on Recent Developments in Control, Automation and Power Engineering (RDCAPE), Noida, India, 26–27 October 2017; IEEE: Piscataway, NJ, USA, 2017; pp. 120–124.
- Lohwanitchai, K.; Jareemit, D. Modeling Energy Efficiency Performance and Cost-Benefit Analysis Achieving Net-Zero Energy Building Design: Case Studies of Three Representative Offices in Thailand. *Sustainability* **2021**, *13*, 5201. [[CrossRef](#)]
- Raj, B.P.; Meena, C.S.; Agarwal, N.; Saini, L.; Hussain Khahro, S.; Subramaniam, U.; Ghosh, A. A Review on Numerical Approach to Achieve Building Energy Efficiency for Energy, Economy and Environment (3E) Benefit. *Energies* **2021**, *14*, 4487. [[CrossRef](#)]
- Badiee, A.; Akhlaghi, Y.G.; Zhao, X.; Li, J.; Yi, F.; Wang, Z. Can whole building energy models outperform numerical models, when forecasting performance of indirect evaporative cooling systems? *Energy Convers. Manag.* **2020**, *213*, 112886. [[CrossRef](#)]
- Carvalho, J.P.; Almeida, M.; Bragança, L.; Mateus, R. BIM-Based Energy Analysis and Sustainability Assessment—Application to Portuguese Buildings. *Buildings* **2021**, *11*, 246. [[CrossRef](#)]
- Homod, R.Z.; Gaeid, K.S.; Dawood, S.M.; Hatami, A.; Sahari, K.S. Evaluation of energy-saving potential for optimal time response of HVAC control system in smart buildings. *Appl. Energy* **2020**, *271*, 115255. [[CrossRef](#)]
- Ascione, F.; Bianco, N.; Iovane, T.; Mauro, G.M.; Napolitano, D.F.; Ruggiano, A.; Viscido, L. A real industrial building: Modeling, calibration and Pareto optimization of energy retrofit. *J. Build. Eng.* **2020**, *101186*. [[CrossRef](#)]
- Büning, F.; Huber, B.; Heer, P.; Aboudonia, A.; Lygeros, J. Experimental demonstration of data predictive control for energy optimization and thermal comfort in buildings. *Energy Build.* **2020**, *211*, 109792. [[CrossRef](#)]
- Kong, X.; Qiao, X.; Yuan, G. Investigation of thermal environment and the associated energy consumption of transportation buildings along the expressways in the cold region of China: A case study. *Energy Built Environ.* **2020**, *1*, 278–287. [[CrossRef](#)]
- Arregi, B.; Garay-Martinez, R.; Astudillo, J.; García, M.; Ramos, J.C. Experimental and numerical thermal performance assessment of a multi-layer building envelope component made of biocomposite materials. *Energy Build.* **2020**, *214*, 109846. [[CrossRef](#)]
- ANSI/ASHRAE. Standard Method of Test for the Evaluation of Building Energy Analysis Computer Programs ANSI/ASHRAE Standard 140-2007; ANSI/ASHRAE: Peachtree Corners, GA, USA, 2010.
- Harish, V.S.K.V.; Kumar, A. A review on modeling and simulation of building energy systems. *Renew. Sustain. Energy Rev.* **2016**, *56*, 1272–1292. [[CrossRef](#)]
- Campisi, D.; Gitto, S.; Morea, D. An evaluation of energy and economic efficiency in residential buildings sector: A multi-criteria analysis on an Italian case study. *Int. J. Energy Econ. Policy* **2018**, *8*, 185.
- Wang, D.; Hu, L.; Du, H.; Liu, Y.; Huang, J.; Xu, Y.; Liu, J. Classification, experimental assessment, modeling methods and evaluation metrics of Trombe walls. *Renew. Sustain. Energy Rev.* **2020**, *124*, 109772. [[CrossRef](#)]
- Ha, T.T.; Feuillet, V.; Waeytens, J.; Zibouche, K.; Thebault, S.; Bouchie, R.; Le Sant, V.; Ibos, L. Benchmark of identification methods for the estimation of building wall thermal resistance using active method: Numerical study for IWI and single-wall structures. *Energy Build.* **2020**, *224*, 110130. [[CrossRef](#)]
- Lencwe, M.J.; Chowdhury, S.P.; Mahlangu, S.; Sibanyoni, M.; Ngoma, L. An Efficient HVAC Network Control for Safety Enhancement of a Typical Uninterrupted Power Supply Battery Storage Room. *Energies* **2021**, *14*, 155. [[CrossRef](#)]
- Franco, A.; Misericocchi, L.; Testi, D. Energy Intensity Reduction in Large-Scale Non-Residential Buildings by Dynamic Control of HVAC with Heat Pumps. *Energies* **2021**, *14*, 3878. [[CrossRef](#)]
- Franco, A.; Bartoli, C.; Conti, P.; Misericocchi, L.; Testi, D. Multi-Objective Optimization of HVAC Operation for Balancing Energy Use and Occupant Comfort in Educational Buildings. *Energies* **2021**, *14*, 2847. [[CrossRef](#)]
- Plörer, D.; Hammes, S.; Hauer, M.; van Karsbergen, V.; Pfluger, R. Control Strategies for Daylight and Artificial Lighting in Office Buildings—A Bibliometrically Assisted Review. *Energies* **2021**, *14*, 3852. [[CrossRef](#)]
- Odiyur Vathanam, G.S.; Kalyanasundaram, K.; Elavarasan, R.M.; Hussain Khahro, S.; Subramaniam, U.; Pugazhendhi, R.; Ramesh, M.; Gopalakrishnan, R.M. A Review on Effective Use of Daylight Harvesting Using Intelligent Lighting Control Systems for Sustainable Office Buildings in India. *Sustainability* **2021**, *13*, 4973. [[CrossRef](#)]

23. Harish, V.S.K.V.; Kumar, A. Reduced order modeling and parameter identification of a building energy system model through an optimization routine. *Appl. Energy* **2016**, *162*, 1010–1023. [\[CrossRef\]](#)
24. Shamsi, M.H.; Ali, U.; Mangina, E.; O'Donnell, J. Feature assessment frameworks to evaluate reduced-order grey-box building energy models. *Appl. Energy* **2021**, *298*, 117174. [\[CrossRef\]](#)
25. Salsbury, T.I. A Survey of Control Technologies in the Building Automation Industry. In Proceedings of the International Federation of Automatic Control World Congress, Prague, Czech Republic, 3–8 July 2005.
26. Harish, V.S.K.V.; Kumar, A. Simulation based energy control and comfort management in buildings using multi-objective optimization routine. *Int. J. Math. Eng. Manag. Sci.* **2020**, *5*, 1324–1332. [\[CrossRef\]](#)
27. Counsell, J.M.; Khalid, Y.A.; Brindley, J. Controllability of buildings: A multi-input multi-output stability assessment method for buildings with slow acting heating systems. *Simul. Model. Pract. Theory* **2011**, *19*, 1185–1200. [\[CrossRef\]](#)
28. Salsbury, T.I. Control performance assessment for building automation systems. In Proceedings of the IFAC Workshop on Energy Saving Control in Plants and Buildings, Bansko, Bulgaria, 3–5 October 2006.
29. Kan, E.M.; Kan, S.L.; Ling, N.H.; Soh, Y.; Lai, M. Multi-zone Building Control System for Energy and Comfort Management. In *Hybrid Intelligent Systems*; Springer International Publishing: Berlin/Heidelberg, Germany, 2016; pp. 44–51.
30. Korkidis, P.; Dounis, A.; Kofinas, P. Computational Intelligence Technologies for Occupancy Estimation and Comfort Control in Buildings. *Energies* **2021**, *14*, 4971. [\[CrossRef\]](#)
31. Counsell, J.M.; Khalid, Y.A. Controllability of Buildings: A multi-input multi-output stability assessment method for buildings with fast acting heating systems. In Proceedings of the CIBSE Technical Symposium, Leicester, UK, 6–7 September 2011.
32. Pasichnyi, O.; Wallin, J.; Kordas, O. Data-driven building archetypes for urban building energy modelling. *Energy* **2019**, *181*, 360–377. [\[CrossRef\]](#)
33. Lamberti, G.; Salvadori, G.; Leccese, F.; Fantozzi, F.; Bluysen, P.M. Advancement on Thermal Comfort in Educational Buildings: Current Issues and Way Forward. *Sustainability* **2021**, *13*, 10315. [\[CrossRef\]](#)
34. Sim, M.; Suh, D.; Otto, M.O. Multi-Objective Particle Swarm Optimization-Based Decision Support Model for Integrating Renewable Energy Systems in a Korean Campus Building. *Sustainability* **2021**, *13*, 8660. [\[CrossRef\]](#)
35. Tsay, Y.S.; Yeh, C.Y.; Chen, Y.H.; Lu, M.C.; Lin, Y.C. A Machine Learning-Based Prediction Model of LCCO₂ for Building Envelope Renovation in Taiwan. *Sustainability* **2021**, *13*, 8209. [\[CrossRef\]](#)
36. Paneru, S.; Foroutan Jahromi, F.; Hatami, M.; Roudebush, W.; Jeelani, I. Integration of Emergy Analysis with Building Information Modeling. *Sustainability* **2021**, *13*, 7990. [\[CrossRef\]](#)
37. Yang, S.; Wan, M.P.; Chen, W.; Ng, B.F.; Dubey, S. Model predictive control with adaptive machine-learning-based model for building energy efficiency and comfort optimization. *Appl. Energy* **2020**, *271*, 115147. [\[CrossRef\]](#)
38. Homod, R.Z. Analysis and optimization of HVAC control systems based on energy and performance considerations for smart buildings. *Renew. Energy* **2018**, *126*, 49–64. [\[CrossRef\]](#)
39. Tang, R.; Wang, S.; Sun, S. Impacts of technology-guided occupant behavior on air-conditioning system control and building energy use. *Build. Simul.* **2021**, *14*, 209–217. [\[CrossRef\]](#)
40. Peng, B.; Zou, H.M.; Bai, P.F.; Feng, Y.Y. Building energy consumption prediction and energy control of large-scale shopping malls based on a noncentralized self-adaptive energy management control system. *Energy Explor. Exploit.* **2020**, *39*, 1381–1393. [\[CrossRef\]](#)
41. Vasak, M.; Banjac, A.; Hure, N.; Novak, H.; Marusic, D.; Lesic, V. Modular Hierarchical Model Predictive Control for Coordinated and Holistic Energy Management of Buildings. *IEEE Trans. Energy Convers.* **2021**, *1*–13. [\[CrossRef\]](#)
42. Zhao, Y.; Genovese, P.V.; Li, Z. Intelligent thermal comfort controlling system for buildings based on IoT and AI. *Future Internet* **2020**, *12*, 30. [\[CrossRef\]](#)
43. Sung, L.Y.; Ahn, J. Comparative analyses of energy efficiency between on-demand and predictive controls for buildings' indoor thermal environment. *Energies* **2020**, *13*, 1089. [\[CrossRef\]](#)
44. Lou, R.; Hallinan, K.P.; Huang, K.; Reissman, T. Smart Wifi Thermostat-Enabled Thermal Comfort Control in Residences. *Sustainability* **2020**, *12*, 1919. [\[CrossRef\]](#)
45. Counsell, J.M.; Khalid, Y.A. Controllability of modern commercial buildings. In Proceedings of the 10th World Renewable Energy Congress, Glasgow, Scotland, 21–25 July 2008.
46. Fallah, M.S.; Bhat, R.B.; Xie, W.F. Optimized control of semiactive suspension systems using H robust control theory and current signal estimation. *IEEE/ASME Trans. Mechatron.* **2012**, *17*, 767–778. [\[CrossRef\]](#)
47. Muir, E.; Bradshaw, A. Control law design for a thrust vectoring fighter aircraft using robust inverse dynamics estimation (RIDE). *Proc. Inst. Mech. Eng. Part G J. Aerosp. Eng.* **1996**, *210*, 333–343. [\[CrossRef\]](#)
48. Harish, V.S.K.V.; Kumar, A. Modeling and simulation of a simple building energy system. In Proceedings of the 2016 International Conference on Microelectronics, Computing and Communications (MicroCom), Durgapur, India, 23–25 January 2016; IEEE: Piscataway, NJ, USA, 2016; pp. 1–6.
49. Golnaraghi, F.; Kuo, B.C. *Automatic Control Systems*; McGraw-Hill Education: New York, NY, USA, 2017; Volume 2, pp. 1–10.
50. Li, X.; Yang, X. Lyapunov stability analysis for nonlinear systems with state-dependent state delay. *Automatica* **2020**, *112*, 108674. [\[CrossRef\]](#)